D37

N79-24038

POTENTIAL MAPPING WITH CHARGED-PARTICLE BEAMS*

James W. Robinson
David G. Tilley
The Pennsylvania State University

SUMMARY

Spacecraft charging produces electric fields near the structures being tested. The calculation of the fields is often difficult because of a complex geometry or a lack of data for dielectric surface potentials. This work seeks experimental methods of mapping the equipotential surfaces near some structure of interest. Such measurements can verify or supplement calculations. The two methods described rely on the detection of charged particles which have traversed the regions of interest and are detected remotely. Whereas techques have been developed previously for use with rotationally symmetric systems, no such restriction is applied in this work. One method is the measurement of ion energies for ions created at a point of interest and expelled from the region by the fields. The ion energy at the detector in eV corresponds to the potential where the ion was created. An ionizing beam forms the ions from background neutrals. The other method is to inject charged particles into the region of interest and to locate their exit points. A set of several trajectories becomes a data base for a systematic mapping technique. An iterative solution of a boundary value problem establishes concepts and limitations pertaining to the mapping problem.

INTRODUCTION

Measurements of electrical potential ultimately depend upon making an observation of a charged particle in the region of interest. Often some mechanical device is also inserted into the region but ideally one would use the smallest charge, the electron, by itself. Then the perturbing effect of the measurement would be at a minimum. This paper describes two approaches for making potential measurements in vacuum where nearby surface charges create the potentials to be measured. The methods both strive to keep the density of test charges to a minimum. All detection equipment is kept out of the region being measured.

The first of these two methods uses the neutral atoms or molecules always present. A collimated ionizing beam of electrons or photons passes through the region and the ions formed are collected and analyzed as they drift out of the region. Typically the pressure will be 10^{-5} Torr and ions will be

*This work was supported by The National Aeronautics and Space Administration under grant number NSG-3166.

detected with a continuous-dynode avalanche detector. The field must be oriented to expel ions for this method to be useable.

The other method requires no background neutrals and it is usable with fields of either polarity. Low-current particle beams are injected into the region of interest with known velocities and entry positions. Exit points are measured. The data from many trajectories may be combined in a iterative calculation that generates a map of the potential in the region probed by the beams.

These two methods have similar purposes but they differ sufficiently in technique that they are described separately in the two major sections of this report. Work is in progress for both methods so that directions of effort are indicated where appropriate.

IONIZATION OF NEUTRALS

This method of measuring potential is simple in concept. If a neutral molecule is located at some point of interest and is ionized by some process, then it will be accelerated by the electric fields and strike a properly positioned detector at reference potential. If the detector can measure the energy of the particle, then that energy (in eV) can be equated to the potential at the original point. A series of measurements point by point provides a map of the region of interest. Several variations of this method are possible but several constraints need to be recognized.

Resolution

The first quantity for which resolution is important is the position of the source point. Ions are generated in some neighborhood having radius a and centered at point r_o. If the potential function to be measured is $\phi(r)$ then its value will be in the range

$$\phi(r) = \phi(r_o) \pm \frac{\partial \phi}{\partial r} (\Delta r + a) \pm \phi_T \qquad (1)$$

where ϕ_T represents a random spread in the ion energies. In most situations, say for $\phi(r) > 1V$, randomness in ion energies may be neglected. However the spread of electron energies may be much higher. Hence ions are the preferred species in many situations but then the gradients must be such as to drive ions toward the detector. The randomness arises from the thermal energy of the neutrals being ionized and from energy imparted by the ionizing agent. The quantity a depends on the width of the particle beam or photon beam which is employed to ionize atoms. This parameter can be made very small by the use of focussed electron beams while with either photons or electrons the required fluxes are small enough that a pair of pin holes will emit a sufficient beam having a diameter of a few millimeters at the point of interest. Finally the effects of beam steering must be considered. Any beam is directed no more accurately than permitted by the reproducibility of

mechanical settings. However this feature should not set a significant limit. Rather the alignment of a system is the critical feature. Also an ionizing electron beam can be deflected by magnetic fields or electrostatic fields so that Δr can be unacceptably large. Increasing electron velocity to decrease Δr is only moderately helpful because above 100 eV, ionization cross sections decrease. When the preceding factors are weighed, the optimum choice for an ionizing agent often will be a collimated beam of photons.

The second quantity to be measured is energy of the ions being detected. After the ions enter the orifice of the detector they must be subjected to some selection process. Either some theshold condition may be imposed such that only those ions with energy exceeding the theshold are recorded, or some system such as a curved-plate analyzer may select particles with energies in a specified band. A threshold device we have used is recommended as it is capable of resolving to within 2% whereas a typical curved-plate system resolves at 7% (ref. 1).

Restrictions

Because of the desire to minimize the effects on the system being measured, one should observe several precautions. First the ionizing beam itself should not strike any surfaces. Otherwise it would modify the surface charge and the potentials at points of interest. Ideally the beam would pass by the structure creating the potential distribution and be absorbed in a dump on the other side from the source.

Another beam effect less easily dismissed is the drifting of electrons to the structure. These electrons are released along with ions at the point of interest. If ions are repelled from the structure, the electrons will be attracted. When neutral gas pressure is uniform throughout the vacuum chamber, ions and electrons are released from all points along the ionizing beam path, yet they are needed only at the one point. Conceivably the neutrals could be concentrated at the region of interest by pumping the chamber to a substantially lower pressure while injecting gas through an appropriately directed nozzle. Then, a beam of neutral atoms would cross paths with the ionizing beam. Use of a sensitive detector is necessary to minimize the charged-particle perturbations. The ionizing beam should be only as intense as needed for observing the response.

When an electron ionizing beam is used, the beam itself perturbs the potentials being measured. If a beam having radius a carries current I where acceleration is through voltage V, then the line charge density, using mks, is

$$\rho_\ell = I\sqrt{\frac{m}{2eV}} \tag{2}$$

The potential at a relative to some reference radius r_o is

$$V(a) - V(r_o) = \frac{\rho_\ell}{2\pi\epsilon_o} \ln (r_o/a) \tag{3}$$

For a typical beam of 1 mm, 10^{-6}A, and 100 V, where we let the reference r_o

correspond to separation between beam and structure (say 0.1 m) we find that $V(a) - V(r_o) = 0.0138V$. This can be ignored.

Electron Beam Experiments

An electron beam source and ion detector were built by David Ross as described in reference 2. These systems are described here and some results are given.

The electron gun consisted of a hot tungsten wire placed behind a pair of apertures. The outer aperture had a diameter of 1.1 mm and it was placed 19.6 mm from the inner aperture having a diameter of 1.4 mm. The apertures were grounded and the filament was biased at -150V to produce a current. As a fine wire probe was moved through the path of the beam, it showed a beam divergence of 2.6° such that at a typical working distance of 10 cm, the beam width was 4.5 mm. Currents, approximately 10^{-8}A, detected by the 1-mm probe wire provided more than adequate ionization.

The test configuration was a conducting right-dihedral angle biased typically at 70V relative to the detector located near the ground plane. Figure 1 shows computed equipotential contours and particle trajectories for the test configuration. The detector moved along the x-axis. The ion source was mounted with two degrees of freedom along the x and y axes and projected a beam more or less parallel to the apex of the wedge. The experiment was essentially two-dimensional.

The basic detector design is illustrated in figure 2. It provides four functions, a measure of beam position at the detector plane, a measure of beam angle, a measure of ion energy, and a means of detecting particles. The detector element was a continous-dynode electron multiplier operated in a pulse-generating mode so that it would indicate the impact of an ion on its input cone. It was followed with a two-stage 10-X amplifier, an oscilloscope which showed pulses, and a counter. For ions to reach the input cone they had to pass through a set of three apertures and a repeller electrode which provided the various types of discrimination. All elements of the system were rigidly mounted in a metal can which could be translated and rotated by mechanical linkages.

The two outer apertures provided the measure of location and angle. Only when both were positioned to correspond with incoming ions would ions enter the inner chamber. The apertures were 12.7 mm apart, the outer had a diameter of 0.76 mm, and the inner, 0.38 mm. The response as a function of angle had a measured half-width of 3°.

The second aperture, the third aperture, and the cylindrical repeller provided the energy discrimination. The repeller was biased positively and created a saddle-point potential between apertures. When particles had sufficient energy to pass over the saddle-point, they continued through the third aperture and were detected. The hole in the third aperture was somewhat larger than the others; this was to avoid loss of particles deflected as they passed over the saddle-point. Figure 3 shows response as a function of bias

voltage on the repeller. Particles at 19.3 eV were repelled by voltages on the tube exceeding 24.1V. The ratio 0.80 of these values corresponds well to 0.79 calculated for the drift-tube, radius-length ratio of 0.45. The drift-tube length was 2.8 cm.

The sample trajectories shown in figure 1 are computer simulations obtained by injecting ions at the detector plane with velocities more or less opposite to those measured. The source point is found to be a very sensitive function of angle, so sensitive that the measure of angle is practically useless. If the position angle measurements were sufficiently accurate, they could be used to corroborate the locations of the source points as determined by the aiming of the electron gun. However our experience has shown that the detector is useful only as an energy measuring instrument. The measure of angles is further complicated by the effects of the magnetic field which causes trajectories to curve.

Our experiences with an electron beam system have suggested two changes in technique. The ionizing beam should consist of photons so that it won't be deflected and the detector should have less angle resolving capability so that the ion beam can be more easily located. However the energy resolution should be maintained.

X-Ray Beam Experiments

A preliminary study of an X-ray beam system has been completed. The electron beam system was adapted to this purpose for a demonstration of concept and now a better X-ray system is being constructed.

For the demonstration of concept the electron source was replaced with an X-ray source which however did not fit well into the available space and could not be steered precisely. Nevertheless a beam was produced and ions were detected. Figure 4 shows detection response for two different orientations of the X-ray beam. Of interest here is the design of the X-ray source. A steel pin biased at +600V drew 0.8 mA of current from a nearby grounded tungsten filament. Soft X-rays emanating from the pin were collimated by a pair of apertures to form a beam which in this case had a radius of 1 cm in the working region.

Under construction are a source having much smaller apertures and a detector having wide-angle response. This combination is expected to provide better resolution.

POTENTIAL MAPPING FROM PARTICLE TRAJECTORIES

Various instances of using beam trajectories to map a rotationally symmetric potential profile have been reported (refs. 3,4) and a general mapping technique has been described where a reasonably dense plasma and magnetic field are required (ref. 5). This work seeks methods of generating potential maps where Laplace's equation is valid and magnetic field is

insignificant. Data characterizing the region of interest are obtained by injecting charged particles (or low-current beams) with known velocities and observing their exit points. A preliminary study of a boundary value problem has provided a useful frame of reference for studies of mapping techniques.

Boundary Value Problem

The analysis of data in the general mapping problem is equivalent, when charge density is low, to solving Laplace's equation. The data set will always be finite, i.e., a finite number of particle trajectories will have been observed, and the map will consequently be approximate. The analyst must decide upon the level of detail he requires and select a data set sufficient for his purposes. He must be cautious not to misuse his data in a manner represented by the function $y = \cos x$ which provides a perfect fit to the set of points ($y_i = 1$, $x_i = 2\pi i$).

The need to solve Laplace's equation led to a preliminary study of a boundary value problem in a context that could be extended to the mapping problem of interest. Being sought was an iterative technique which would converge toward a solution as precise as boundary specifications would justify. Convergence was accomplished by comparing the approximate solution with boundary constraints and then perturbing the solution to improve the match. The procedure was developed for boundary conditions specified as values of potential on a set of points spaced more or less uniformly on the boundary.

The key to the method is the choice of perturbing function. Let the estimated solution ϕ_e be of a functional form known to satisfy Laplace's equation. Also let some perturbation ϕ_d be a solution of Laplace's equation which decreases with distance from some singular point. Then the sum $\phi = \phi_e + \phi_d$ must be a solution because of the superposition principle. When ϕ_d is properly chosen, ϕ will match the boundary conditions more closely than ϕ_e does and a convergent process can be developed. The perturbation must be localized to a small portion of the boundary so that when an improvement is made in the match for that portion, the other portions will not be changed much. Also the singularity must be located outside of the region of interest. Consequently the singularity will be placed outside of but near to the boundary where matching is to be improved. The perturbation can be that of a single charge, a dipole, or a higher order pole but we have chosen to work exclusively with dipoles. They are reasonably localized without being overly difficult to manipulate.

With respect to some location and preferred direction, we may describe a dipole as

$$\phi_d = \mu (\cos\alpha)/\rho^2 \qquad (4)$$

where μ is the strength, α is the orientation of the field point, and ρ is the distance of the field point. This is the potential function in 3 dimensions for a dipole consisting of plus and minus point charges closely spaced.

However for 2-dimensional work the choice should be

$$\phi_d = \mu\ (\cos\alpha)/\rho \tag{5}$$

which represents the potential for plus and minus line charges. In either case the separation between charges is small compared with ρ and the dipole is a singularity. When a 2-dimensional dipole is located at (x_d,y_d) and a field point at (x,y), then ϕ_d is given by

$$\phi_d = \frac{\mu\ \cos\beta\,(x-x_d) + \mu\ \sin\beta\ (y-y_d)}{(x-x_d)^2 + (y-y_d)^2} \tag{6}$$

where β is the orientation of the dipole measured relative to the x-direction. Though we need not restrict β, we find it convenient to choose $\cos\beta = -\ x_d/r_d$ and $\sin\beta = -\ y_d/r_d$ where r_d is the displacement of the dipole from the origin. Thus when μ is positive, the positive side of the dipole faces the origin and ϕ_d is given by

$$\phi_d = -\ \frac{\mu}{r_d}\ \left(\frac{x_d(x-x_d) + y_d(y-y_d)}{(x-x_d)^2 + (y-y_d)^2}\right) \tag{7}$$

The dipole is placed so as to produce a desired perturbation in ϕ_e. Let the origin be at the centroid of a closed boundary curve (2-dimensions) whose radius is a single-valued function of angle. Assume that for some boundary point (R,θ) the discrepancy between ϕ_e and the specified boundary condition is largest of all discrepancies and then place the dipole on the same radius θ at $r_d > R$. See figure 5. At (R,θ), equation (7) reduces to

$$\phi_d(R,\theta) = \mu/(r_d-R) \tag{8}$$

and we are assured that the largest perturbation on the boundary will occur at (R,θ), at least if the radius of the boundary does not change greatly from one point to the next. If ϕ_b represents the specified boundary condition we require that

$$\phi_b(R,\theta) = \phi_e(R,\theta) + \mu/(r_d-R) \tag{9}$$

and then we calculate ϕ at all points of interest in the region. Even with β previously specified, we must exercise a choice of either r_d or μ.

When the dipole is placed far from the boundary its strength must also be large and its influence extends to a large portion of the bounded region. In the limit as r_d and μ approach infinity, the dipole affects all points equally and in fact shifts all points by a constant. At the other extreme, that of close placement, the effect of the dipole is very localized. The choice of position represents compromises between speed and accuracy of the solution. When boundary conditions are specified as a set of points, they can be satisfied easily by placing a small dipole very near to each point. However this solution is not desirable because it will bear little resemblance to the relatively smooth boundary function likely to have been implied by the set of boundary points. Furthermore various solutions may be obtained

as different choices of μ and r_d are made. When a minimum distance r_d-R is specified, a given dipole can be forced to influence several boundary points and the boundary function will be smooth. A solution will still not be unique but various solutions will differ only in small amounts. We have found practically that r_d-R should be at least as large as the distance between neighboring boundary points. A useful criterion expressed in terms of the number of boundary points n is that

$$r_d - R = RG/n \tag{10}$$

where typically $G \geq 2\pi$.

Convergence can be obtained by specifying that all dipoles will be a given distance from the boundary. In this case the number of dipoles is equal to the number of boundary points though a given dipole strength may be the sum of contributions from several iterations. However convergence may be faster if some criterion in introduced for picking distance. Figure 5 illustrates two situations in terms of discrepancies indicated by each point where we define discrepancy at the ith point by

$$d_i = \phi_{bi} - \phi_{ei} \tag{11}$$

When several adjacent points have discrepancies of the same sign, the dipole should be far enough away that it will perturb all of those points. On the other hand, when discrepancies alternate in sign, the dipole should be close. Noting that (R,θ) locates the point of absolute maximum discrepancy, we let (R',θ') represent the nearest point for which the discrepancy is of the opposite sign. Letting d_a be the average absolute discrepancy and T be some constant $0 < T < 1$, we can select r_d so that

$$\phi_d(R',\theta') = \pm T\, d_a \tag{12}$$

The sign is chosen to be the same as for $\phi_d(R,\theta)$. This requirement on $\phi_d(R',\theta')$ forces a choice of r_d that is sensitive to the polarities of nearby discrepancies, but retrictions are necessary. When T is specified as being small, the value of r_d may not satisfy equation (10) which must be given priority. When T is large the convergence will be slow and perhaps nonexistent. The benefits of introducing equation (12) are relatively minor.

Though, in concept, dipole perturbation alone should suffice for finding a solution, some auxiliary operations have been found to be useful. These are rotating, shifting, and scaling of the estimated potential function. As an initial estimated potential one may simply assume that $\phi = x$. However if say potential increases more or less as y, then a preliminary rotation of 90° is appropriate. One might subsequently replace ϕ_e by $\phi'_e = \phi_e + b$ where b represents a shift. In terms of discrepancies b is calculated from

$$b = -\sum_i d_i/n$$

When shifting has been done the average potential is

$$\phi_a = \sum_i \phi'_{ei}/n = \sum_i \phi_{bi}/n \qquad (14)$$

Finally a scaling factor can be determined:

$$c = \sum_i |\phi_{bi}-\phi_a| \; / \; \sum_i |\phi'_{ei}-\phi_a| \qquad (15)$$

The potential ϕ' is replaced by a scaled potential:

$$\phi'' = c\,(\phi'-\phi_a) + \phi_a \qquad (16)$$

For our work, each dipole addition has been preceded with both shifting and scaling operations.

Details of the method have been explained for the 2-dimensional case, though no assumptions have been introduced which would limit the method from being applied in 3 dimensions. The number of boundary points would be larger and correspondingly more dipoles would be required.

Potential has been found at points inside of a square by the method of dipole perturbations. The test problem is specified in figure 6 which shows 20 boundary points uniformly distributed in angle. All points on the bottom side of the square were assigned a potential of 0 and the others a potential of 10. Potentials were calculated for boundary points and for an array of internal points layed out in polar coordinates. Equipotential contours were then plotted as shown in figure 7. Points on the equipotentials were found by linearly interpolating along a straight line between array points; some of the irregularities noted in the figure may be attributed to the approximation made in the interpolation. Potential intervals between curves are 0.25V. This example required 214 dipoles where the convergence criterion was that $\Sigma|d_i| < 0.00001$, though a much less stringent criterion could have been used.

Potential Mapping

The transition from the boundary value problem to the particle-trajectory problem is accomplished by using trajectory data in place of boundary data when synthesizing the potential function. The general approach is to sum contributions of numerous dipoles placed outside the region of interest such that simulated particle trajectories in the region match the observed trajectories. As in the boundary value problem, the solution is not unique and the data must not be overextended.

The problem has been defined in two dimensions with reference to a line along which both beam source and detector move. A beam is injected into the space above the line, repelled, and returned to the line where its exit position is monitored. Measurements are of entrance position, entrance velocity, and exit position for as many selected beams as required by the application. The beam can be of either electrons or ions. A computer simulation uses a known potential distribution that can be produced experimentally with a set of parallel fins as illustrated in figure 8. The base line is at ground potential, all fins are equally biased, and equipotential,

lines have been computed for the configuration. Shown in the figure are several simulated particle trajectories. The potential ϕ can be found with a conformal mapping from a flat plane given by

$$\phi = \text{Imag}\,[\sin^{-1}(e^{c})] - \text{Imag}\,[\sin^{-1}(e^{w})],\ w = (c-y) + ix \quad (17)$$

The zero potential line does not exactly match the x-axis but the error is small enough to be ignored if c exceeds 2. The fin spacing is π.

Experimental trajectory data are being sought to test the procedure but they can also be simulated with a trajectory tracing program. In fact the simulation will permit an assessment of what experimental errors can be tolerated. Both for providing simulated data and for use in the potential mapping procedure, a tracing routine developed by DeVogelaere (ref. 6) has been programmed. The routine requires fields to be calculated at specific points on the trajectory and when potential is specified on a discrete set of points, Newton's interpolation procedure (ref. 7) is used.

The scenario of the simulation follows three steps. First the potential illustrated in figure 8 is calculated for a square array of points. The simulated particles are injected into the array, trajectories are traced, and exit points are recorded. Finally these simulated trajectories are used as a basis for generating various potential maps which can be compared with the original array to assess the effectiveness of the mapping procedure.

The map is constructed by placing dipoles above the region being mapped. Let the vertical placement y_d exceed the maximum range of the map so that the singularity does not fall in that range. There is a requirement that the reference plane have a fixed potential so that a dipole placed at (x_d, y_d) must be balanced with its image at $(x_d, -y_d)$. An original estimated potential function $\phi = ay$ is then perturbed by the placement of dipoles in pairs until some convergence criterion is met.

Work in progress presently deals with the process of selecting dipoles. Shown in figure 9 is a map which has partially converged after the placement of 8 relatively weak dipoles. The convergence is quite slow and subject to instabilities if it is speeded up. For this particular map, each dipole selection was based on the trajectory which deviated most from the desired exit point. This approach, analogous to the correction of the worst point in the boundary value problem, has some basic flaws which are best overcome by considering several neighboring trajectories in making the choice of a dipole. For example if two trajectories at different x-values have deviations of opposite sign then a dipole might be placed at some x_d intermediate between them. Choice of y_d is related to how many trajectories are to be substantially modified by the dipole. In any case dipoles are to be kept at least as far above the boundary as the trajectories are spaced from each other.

CONCLUDING REMARKS

Measurements show that a beam of electrons or photons can ionize enough neutrals at 10^{-5} Torr that they can be detected by a continuous-dynode electron multiplier behind collimating pinholes. The energy of the ions when detected is a direct measure of the potential where they were created. The photon beam has the advantage that it can be directed to the desired spot along a straight line whereas an electron beam curves in the electric and magnetic fields usually present. Though the ion detector was designed to provide spacial and angular resolution of the ion trajectories, it need only resolve energy.

A method of solving Laplace's equation is described where the final solution is the sum of some initial estimate and the contributions of selected dipoles placed outside the region of interest. A preliminary calculation is based upon the specification of potentials on a discrete set of boundary points. This result is then extended to the use of particle trajectory data in place of boundary potentials. Work in progress seeks to identify efficient schemes of picking dipoles from an analysis of trajectory data so that potential maps may be generated.

REFERENCES

1. Green, D. W. and Whalen, B. A.: Ionospheric Ion Flow Velocities From Measurements of the Ion Distribution Function Technique. Journal of Geophysical Research 79, pp. 2829-30, July 1, 1974.

2. Ross, David P.: Ion Tracking in an Electrostatic Potential Distribution. The Pennsylvania State University, NASA CR-156983, May 1978.

3. Stallings, C. H.: Journal of Applied Physics 42, p. 2831, 1971.

4. Black, W. M. and Robinson, J. W.: Measuring Rotationally Symmetric Potential Profiles with an Electron-Beam Probe. Journal of Applied Physics 45:6 pp. 2497-2501, June 1974.

5. Reinovsky, R. E. et al: Performance of a Feedback Controlled Electrostatic Analyzer for Use with an Ion Beam Probe Diagnostic System. IEEE Trans. on Plasma Science PS-3, 194-200, December 1975.

6. Booth, Andrew D.: Numerical Methods, Butterworths 1966, 3rd ed., p. 71.

7. Steffensen, J. F.: Interpolation, Williams and Wilkins 1927, pp. 14-34, 203-224.

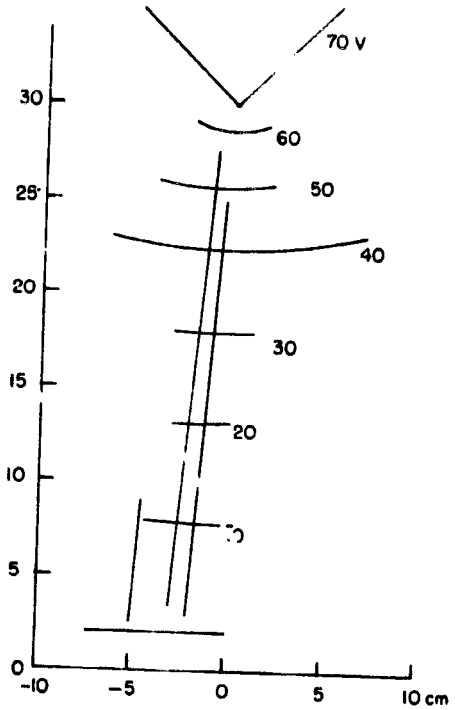

Figure 1. - Simulated trajectories for ionizing electron beam experiment.

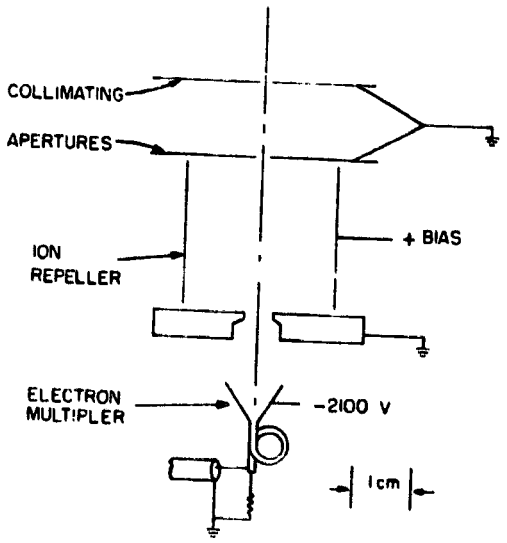

Figure 2. - Ion detection system.

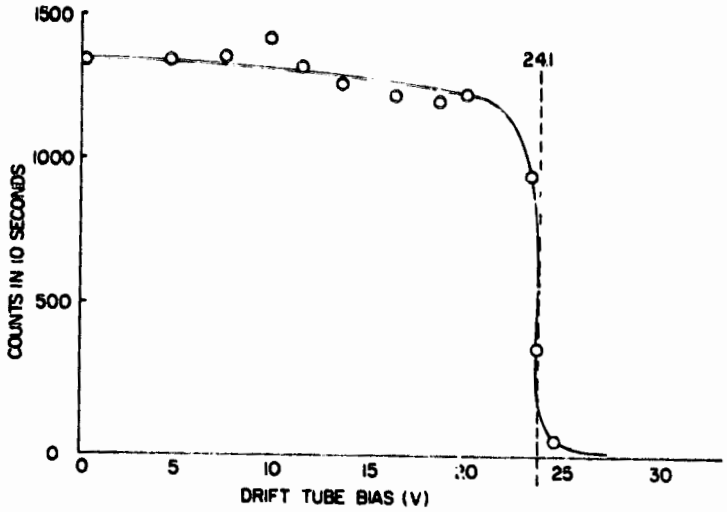

Figure 3. - Detector response to 19.3-eV ions.

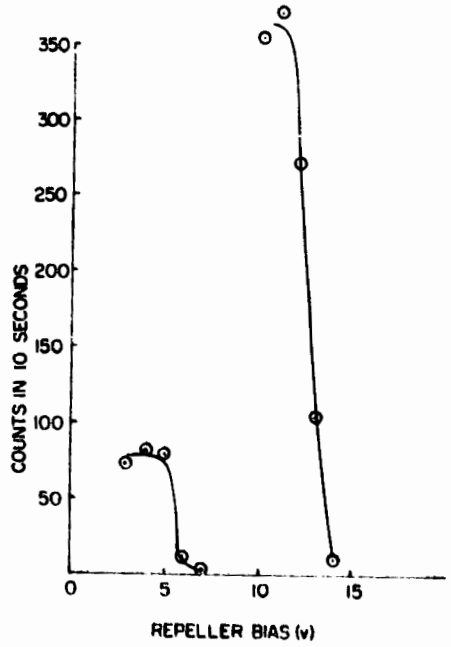

Figure 4. - Detector responses for two X-ray beam positions.

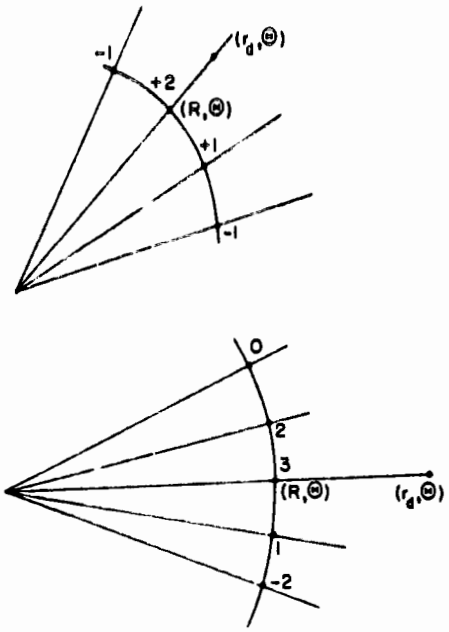

Figure 5. - Dipole placement, with numerals showing discrepancies.

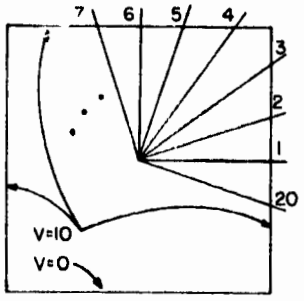

Figure 6. - Assignment of boundary conditions at 20 points.

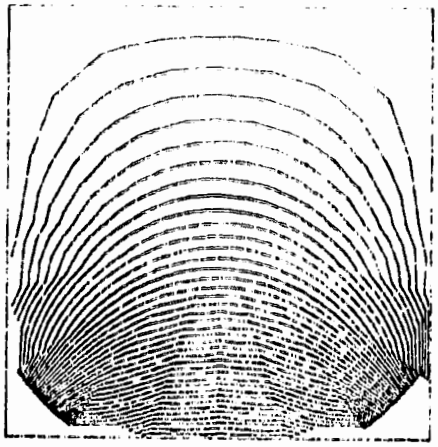

Figure 7. - Equipotential lines for boundary value problem.

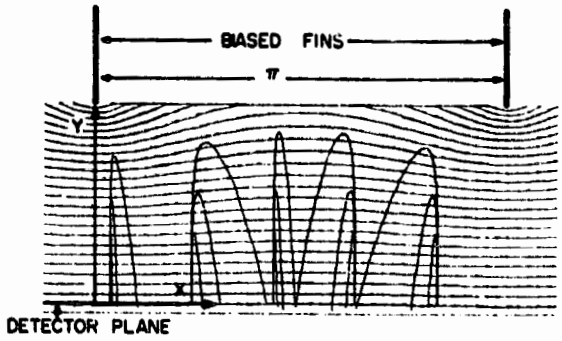

Figure 8. - Test potential and simulated trajectories.

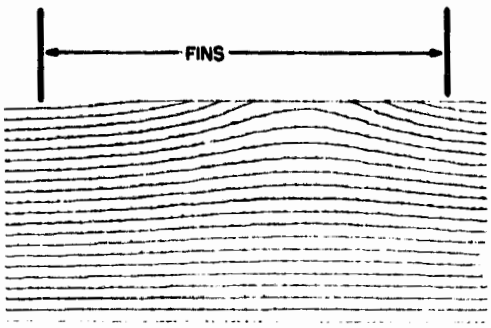

Figure 9. - Partially converged potential map based on trajectory data.